INTERNATIONAL JOURNAL FOR NUMERICAL METHODS IN FLUIDS
Int. J. Numer. Meth. Fluids **28**: 1139–1158 (1998)

A NAVIER–STOKES SOLVER FOR COMPLEX THREE-DIMENSIONAL TURBULENT FLOWS ADOPTING NON-LINEAR MODELLING OF THE REYNOLDS STRESSES

V. BOTTE, A. TOURLIDAKIS* AND R. L. ELDER

Department of Turbomachinery and Mechanical Engineering, School of Mechanical Engineering, Cranfield University, Cranfield, Bedford, UK

SUMMARY

A non-linear modelling of the Reynolds stresses has been incorporated into a Navier–Stokes solver for complex three-dimensional geometries. A k–ε model, adopting a modelling of the turbulent transport which is not based on the eddy viscosity, has been written in generalised co-ordinates and solved with a finite volume approach, using both a GMRES solver and a direct solver for the solution of the linear systems of equations. An additional term, quadratic in the main strain rate, has been introduced into the modelling of the Reynolds stresses to the basic Boussinesq's form; the corresponding constant has been evaluated through comparison with the experimental data. The computational procedure is implemented for the flow analysis in a 90° square section bend and the obtained results show that with the non-linear modelling a much better agreement with the measured data is obtained, both for the velocity and the pressure. The importance of the convection scheme is also discussed, showing how the effect of the non-linear correction added to the Reynolds stresses is effectively hidden by the additional numerical diffusion introduced by a low-order convection scheme as the first-order upwind scheme, thus making the use of higher order schemes necessary. © 1998 John Wiley & Sons, Ltd.

KEY WORDS: non-linear Reynolds stresses; k–ε turbulence model; higher-order convective scheme; pressure correction; direct sparse matrix solver; incompressible duct flows

1. INTRODUCTION

Simple turbulence models are still the most widely used models in the study of turbulent flows in complex, three-dimensional geometries. In particular, the k–ε method, that has been proven to provide a good balance between computational effort and accuracy of the results, could be defined as the standard choice for turbulence modelling and is still mostly used in the original form proposed by Jones and Launder [1] and Launder and Spalding [2]. In many engineering applications, however, much more approximate algebraic methods, such as the mixing length, are still widely used, especially for industrial applications.

Recently, second-moment turbulence transport closure has been used in conjunction with the general non-orthogonal co-ordinate system, as necessary to the study of complex ge-

* Correspondence to: Department of Turbomachinery and Engineering Mechanics, School of Mechanical Engineering, Cranfield University, Cranfield, Bedford MK43 OAL, UK. Tel: + 44 1234 754653; Fax: + 44 1234 750728; E-mail: A.Tourlidakis@cranfield.ac.uk

CCC 0271–2091/98/181139–20$17.50

Received November 1996
Revised June 1997

ometries [3]. Although it is presumably superior to eddy viscosity models, in three dimensions this approach requires the solution of six quite complex equations for the transport of the components of the Reynolds stresses tensor. Additional problems are introduced from the possibility of decoupling between the velocity field and the Reynolds stresses when using a collocated grid.

Most researchers prefer to keep the simple formulation of the k–ε model while trying to increase the accuracy by introducing additional terms and/or modifying the value of the modelling constants in order to take into account the influence of effects such as curvature or rotation. Empirical observations or simplified analyses of the Reynolds stresses equations are often used (see, e.g. the review on turbulence models for complex flows from Lakshminarayana [4]).

The present study originated from the necessity of obtaining a k–ε model for complex, three-dimensional flows, that could be used in conjunction with a completely generic formulation for the Reynolds stresses, and is therefore not based on the linear Boussinesq's approximation, as in the standard formulation.

A modified k–ε model is obtained using a different approach for the modelling of the turbulent diffusive transport term, based on formulas proposed by Hanjalic and Launder [5] for the transport of the Reynolds stresses, instead of the common approach that uses the eddy viscosity and a turbulent Prandtl number. In the existing literature there has been a relatively limited use of these formulas, generally in very simplified cases, and never in general non-orthogonal co-ordinates, to model complex three-dimensional flows using a Navier–Stokes solver. The model obtained is much less diffusive than the original one and is not any more dependent on Boussinesq's assumption; furthermore it can be used in conjunction with different models for the Reynolds stresses.

A non-linear formulation for the Reynolds stresses has then been tested with this modified k–ε model. Non-linear k–ε models that are not based on an eddy viscosity formulation have been proposed by several authors in the past, notably by Baker and Orzechowski [6] and Speziale [7], but again, were tested only in very simplified and particular cases. The model adopted in the present work is both similar to the one proposed by Baker and Orzechowski and a simplified version of Speziale's model, the non-linear term being added as a correction to Boussinesq's formulation. However, as opposed to the previous models, it has been incorporated into a completely general Navier–Stokes solver, adopting generalised co-ordinates for arbitrarily shaped three-dimensional geometries.

2. GOVERNING EQUATIONS

The turbulent diffusive transport of a species ϕ is usually written in accordance with Fick's law, as a function of the eddy viscosity μ_t and of a turbulent Prandtl number σ_ϕ, as

$$\frac{\mu_t}{\sigma_\phi}\underline{\nabla}\phi. \tag{1}$$

Hanjalic and Launder [5] derived, from the study of the transport equations for the Reynolds stresses, the following expressions (in Cartesian co-ordinates) for the modelling of the turbulent diffusive transport of k and ε, respectively:

$$-\frac{1}{2}\rho\overline{u_i' u_i' u_j'} = C_s \frac{k}{\rho\varepsilon}\left(\tau_{il}^R \frac{\partial \tau_{ij}^R}{\partial x_l} - \rho\tau_{jl}^R \frac{\partial k}{\partial x_l}\right), \tag{2}$$

$$-\rho\overline{u_j'\varepsilon'} = C_\varepsilon \rho \frac{k}{\varepsilon}\overline{u_j' u_l'}\frac{\partial \varepsilon}{\partial x_l} = -C_\varepsilon \frac{k}{\varepsilon}\tau_{jl}^R \frac{\partial \varepsilon}{\partial x_l}, \tag{3}$$

where C_s and C_ε are closure constants, and τ_{ij}^R are the components of the Reynolds stresses tensor. A k–ε model based on these assumptions can be written, in generalised co-ordinates, as follows:

Momentum equations:

$$\frac{1}{J}\frac{\partial}{\partial \xi_r}(\rho U_r u_i) = \frac{\partial P}{\partial \xi_r}\frac{\partial \xi_r}{\partial x_i} + \frac{1}{J}\frac{\partial}{\partial \xi_r}\left[J\mu g^{rs}\frac{\partial u_i}{\partial \xi_s} + J\frac{\partial \xi_r}{\partial x_j}\tau_{ji}^R\right], \quad i = 1, 2, 3. \tag{4}$$

Transport equation for k:

$$\frac{1}{J}\frac{\partial}{\partial \xi_r}(\rho U_r k) = \frac{1}{J}\frac{\partial}{\partial \xi_r}\left[J\mu g^{rs}\frac{\partial k}{\partial \xi_s} + JC_s\frac{k}{\rho\varepsilon}\frac{\partial \xi_r}{\partial x_j}\left(\tau_{il}^R\frac{\partial \xi_s}{\partial x_l}\frac{\partial \tau_{ij}^R}{\partial \xi_s} - \rho\tau_{jl}^R\frac{\partial \xi_s}{\partial x_l}\frac{\partial k}{\partial \xi_s}\right)\right] + G - \rho\varepsilon. \tag{5}$$

Transport equation for ε:

$$\frac{1}{J}\frac{\partial}{\partial \xi_r}(\rho U_r \varepsilon) = \frac{1}{J}\frac{\partial}{\partial \xi_r}\left[J\mu g^{rs}\frac{\partial \varepsilon}{\partial \xi_s} - JC_\varepsilon\frac{k}{\varepsilon}\frac{\partial \xi_r}{\partial x_j}\tau_{jl}^R\frac{\partial \xi_s}{\partial x_l}\frac{\partial \varepsilon}{\partial \xi_s}\right] + \frac{\varepsilon}{k}(C_{\varepsilon 1}G - C_{\varepsilon 2}\rho\varepsilon), \tag{6}$$

where $C_{\varepsilon 1}$ and $C_{\varepsilon 2}$ are closure constants, and the production of turbulence energy is given by

$$G = \tau_{ij}^R\frac{\partial u_i}{\partial \xi_r}\frac{\partial \xi_r}{\partial x_j},$$

3. MODELLING OF THE REYNOLDS STRESSES

The k–ε method presented in the previous section allows the use of an arbitrary modelling of the Reynolds stresses. The usual modelling of the Reynolds stresses is based on Boussinesq's assumption:

$$\tau_{ij}^R = \mu_t\left[\left(\frac{\partial u_j}{\partial x_i} + \frac{\partial u_i}{\partial x_j}\right) - \frac{2}{3}(\underline{\nabla}\cdot\underline{V})\delta_{ij}\right] - \frac{2}{3}\rho k\delta_{ij}, \tag{7}$$

where $\mu_t = C_\mu\rho k^2/\varepsilon$ is the eddy viscosity and the constant C_μ is assumed to be a scalar, in the assumption of isotropic turbulence. This linear relationship between stresses and strain produces acceptable results for thin shear flows, but fails to determine any form of turbulence anisotropy. In reality, anisotropy is significant for three-dimensional flows even in plane thin shear layers, while streamline curvature introduces additional complications, due to the remarkably strong interaction between curvature strain and the normal stresses [8].

Methods based on the linear modelling (Equation (7)) generally give inaccurate predictions for the normal Reynolds stresses, and are incapable of properly predicting flows where the normal Reynolds stresses play an important role, such as in recirculation and secondary flows. For example, adopting the modelling of Equation (7), it is impossible to predict the presence of secondary flows in fully developed turbulent flows in a rectangular duct, a physical effect that has been observed experimentally [9]. Speziale [10] has proven that in order for secondary flows to occur in a rectangular duct, the axial mean velocity must give rise to a difference in the transverse normal stresses: $\tau_{xx}^R \neq \tau_{yy}^R$ (z being the axial direction), while in this case the modelling (7) produces $\tau_{xx}^R = \tau_{yy}^R$.

A simple way to overcome the limitations of Boussinesq's assumption, both in the prediction of anisotropy and in the sensitivity of the stress components to secondary strains associated with curvature, is to maintain the basic assumption of the dependence of the Reynolds stresses on the strain rate tensor, but adopting a non-linear, e.g. quadratic or cubic, relationship. Several quadratic stress–strain relationships have been proposed in recent years, by Baker and Orzechowski [6], Speziale [7], Nosizima and Yoshizawa [11], Rubinstein and Barton [12], Myong and Kasagi [13], and Shih *et al.* [14]. Craft *et al.* [15] presented a cubic stress–strain relationship, claiming that no quadratic form is able to correctly account for the effects of streamline curvature on the turbulent stresses. It is interesting to note that most of these formulations are extremely similar, while presenting very different values for the modelling coefficients (see Reference [15]), depending on the flows that have been chosen to evaluate the recommended constants. In effect, all the models appear to be calibrated by reference to a certain number of simple flows, mostly two-dimensional, so that none of the models can guarantee an accurate resolution of anisotropy for arbitrary, complex three-dimensional flows, as has been shown in several assessments of turbulence models (e.g. Reference [16]). This apparent lack of universality, together with the complexity of the formulations proposed so far, especially if written in generalised co-ordinates, complicates the choice of a modelling of the Reynolds stresses for practical three-dimensional computations.

In this work, in order to test the ability of a non-linear stress–strain relationship to accurately predict three-dimensional flows with streamline curvature, a correction, quadratic in the strain rate, will be added to the linear relation (7). The formulation adopted for the Reynolds stresses must satisfy the consistency condition

$$\tau_{11}^R + \tau_{22}^R + \tau_{33}^R = -2\rho k,$$

which can be satisfied by taking

$$\tau_{ij}^R = -\frac{2}{3}\rho k \delta_{ij} + \tau_{ij}^0,$$

where τ_{ij}^0 is a traceless tensor. In addition, the model must be frame-indifferent, i.e. it must have the same form whether or not the frame of reference is inertial. This can be achieved by allowing τ_{ij}^R to depend only on the frame-indifferent parts of the tensor $\underline{\nabla} \otimes \underline{V}$ and its derivatives [17].

Defining D_{ij} as twice the main strain rate tensor (frame indifferent part of $\underline{\nabla} \otimes \underline{V}$:

$$D_{ij} = \frac{\partial u_j}{\partial x_i} + \frac{\partial u_i}{\partial x_j} = \frac{\partial u_j}{\partial \xi_s}\frac{\partial \xi_s}{\partial x_i} + \frac{\partial u_i}{\partial \xi_s}\frac{\partial \xi_s}{\partial x_j}, \tag{8}$$

the simplest quadratic formulation, that satisfies both conditions and the symmetry requisites, can be written as

$$\tau_{ij}^R = -\frac{2}{3}\rho k \delta_{ij} + C_\mu \rho \frac{k^2}{\varepsilon} D_{ij} + C\rho \frac{k^3}{\varepsilon^2}\left(D_{im}D_{mj} - \frac{1}{3} D_{mn}D_{mn}\delta_{ij}\right), \tag{9}$$

which, as can be easily seen, corresponds to Speziale's model without the additional term containing the frame-indifferent part of the convective derivative of $\underline{\nabla} \otimes \underline{V}$ (term containing the Oldroyd derivative).

For the turbulent flow in a rectangular duct the simplified formulation (9) still introduces the anisotropy between the normal stresses that are necessary to produce secondary flows: substituting $\underline{V} = w\underline{k}$ into Equation (9), with $\underline{k}$ the direction of the z-axis and w the corresponding velocity, the following difference between the transverse normal stresses is obtained:

$$\tau_{yy}^R - \tau_{xx}^R = C\rho \frac{k^3}{\varepsilon^2}\left[\left(\frac{\partial w}{\partial y}\right)^2 - \left(\frac{\partial w}{\partial x}\right)^2\right],$$

which is perfectly equivalent to the result obtained by the complete Speziale's formulation. At the same time, the proposed modelling fails to correctly predict the normal stresses in a fully developed two-dimensional channel flow; in this case, supposing that the flow direction coincides with the x-axis, the modelling (9) predicts $\tau_{xx}^R = \tau_{yy}^R$, which is contradicts the experimental observations [18].

The proposed simplified modelling (9), although obviously lacking in universality, provides a very simple way to test the effects of the introduction of quadratic terms in the strain rate in the formulation of the Reynolds stresses for the prediction of three-dimensional complex flows. The constant C, on which the contribution of the non-linear part depends, will be obtained through comparison with the experimental data available for a three-dimensional geometry with strong streamline curvature.

4. THE SOLUTION PROCEDURE

A finite volume procedure for a collocated grid has been utilised, using a pressure correction procedure obtained by extending the classical SIMPLE method of Patankar and Spalding [19] to the case of generalised co-ordinates and non-staggered grid [20]. For the three Cartesian velocity components, k, ε and the pressure correction, the result of the discretisation of the governing equations for a control volume around the generic grid node P is a discrete equation which has the typical form

$$a_P \phi_P = \sum_{K=\mathrm{E,W,N,S,F,B}} a_K \phi_K + S_P, \tag{10}$$

where E, W, N, S, F, B are the surrounding nodes in the computational space.

The coefficients of the transport equations are evaluated using the first-order upwind scheme as a convection scheme, while the contribution of higher order schemes is added to the source term through deferred correction. All of the terms corresponding to the modelling of the turbulent diffusion are also treated explicitly and added to the source. The values of the diffusion and the Reynolds stresses in the grid points close to the solid walls have both been assigned using the classical wall function approach [2].

Writing Equation (10) for all the n grid points of the domain, a linear system of n equations is obtained for each variable. The matrix of the coefficients of such systems is not symmetric (although symmetric in shape) and is not positive definite; although the elements of the matrix are only non-zero in a very narrow band, the storing of the band of the matrix could be prohibitive for three-dimensional problems of engineering interest.

In this study a conjugate gradient-like iterative solver, using a sparse column format for the storing of the non-zero entries of the matrix, has been used. A GMRES procedure [21] has been adopted for solution of all systems of equations, except the one obtained for the pressure correction. In the solution of the system of equations for the pressure correction, GMRES presents an extremely slow convergence due to the ill-conditioning of the matrix of the coefficients. The use of a higher order scheme, in particular if used in conjunction with a flux-limiter, appears to cause a great deterioration in the convergence of GMRES in the solution of the pressure correction equation, so that the solver cannot guarantee an accurate solution of the system [22]. Several preconditioning techniques (nominally: Jacoby preconditioning, incomplete Cholesky factorisation, incomplete LU factorisation, truncated Neumann

and least squares polynomial expansions) have been tested, but all have failed to produce any improvement in the convergence of GMRES for this particular case.

Instead, a direct solver, also adopting a sparse column format for the storing of the coefficients, has been used for the pressure correction system, thus permitting a very accurate solution of this system (down to machine accuracy). The structure of the matrix is preprocessed prior to the numerical factorisation, adopting a reordering of the row and columns based on the multiple degree algorithm [23], which reduces the amount of fill-in created during the factorisation. The system is then solved using the multifrontal method [24] which uses update matrices to carry the intermediate results from the variables being eliminated to the variables that are not yet processed. Therefore, before the elimination of a variable, update matrices corresponding to previously eliminated variables are assembled to form the current frontal matrix. The partial factorisation of the current frontal matrix is then carried out, and its update matrix is generated.

The solution procedure is schematically represented in Figure 1.

It is important to note that the use of a turbulence model, which is not based on the eddy viscosity, for the modelling of the turbulent diffusive transport causes a deterioration in the stability of the numerical procedure.

The numerical tests show that the proposed k–ε formulation introduces considerably less numerical diffusion than the formulation based on an eddy viscosity. In particular, the modelling (1) of the turbulent diffusion term appears to be the main cause of the excessive diffusivity of the usual eddy viscosity formulation. As a consequence, higher order convection schemes are more effective with the formulation proposed in this study but, on the other hand, the procedure is less stable and could require a lowering of the underrelaxation parameters with respect to the values used for the eddy viscosity formulation.

In addition to this problem, the balance between the implicit and explicit part of the transport equations could be drastically modified if all of the turbulent diffusion term is included in the source, as this term usually contributes to the coefficients of the equations.

5. THE CONVECTION SCHEME

Particular care must be given to the treatment of the convection. Note that the modelling of the Reynolds stresses will principally affect the diffusion term in the governing equations; therefore, the effect of the quadratic term on the diffusion, which has been introduced as a correction to the linear formulation of the Reynolds stresses and presumably contributes less to the turbulent diffusion term, could be hidden by the additional numerical diffusion introduced by a low-order convection scheme, such as the first-order upwind scheme. For this reason a higher order scheme must be used.

A third-order convection scheme (Leonard's QUICK [25]) has been adopted in conjunction with the solution procedure described above, for all of the transport equations (the symbols used are defined in Figure 2):

$$\phi_w = \frac{1}{2}(\phi_C + \phi_D) - \frac{\Delta\xi_D^2}{8}(\phi_{\xi\xi})_C + \frac{\Delta\eta^2}{24}(\phi_{\eta\eta})_C + \frac{\Delta\zeta^2}{24}(\phi_{\zeta\zeta})_C, \tag{11}$$

where transverse terms have been introduced to take the curvature of the streamlines into account, and $\Delta\eta$ and $\Delta\zeta$ are the cell dimensions in the cross directions. Numerical tests have shown an important effect of the transverse terms in the accuracy of the results. A flux limiter, following the universal limiter constraints proposed by Gaskell and Lau [26], has been used in conjunction with the QUICK scheme.

Note that the grid in the computational space is chosen with a volume distribution similar to the one in the physical space, in order to avoid large values of the metric coefficients, which could generate higher truncation errors in the summations. Therefore, all of the derivatives appearing in the governing equations are evaluated with non-uniform grid formulas, e.g.

$$(\phi_{\xi\xi})_C = \frac{2}{\Delta\xi_D + \Delta\xi_C}\left(\frac{\phi_D - \phi_C}{\Delta\xi_D} - \frac{\phi_C - \phi_U}{\Delta\xi_C}\right). \tag{12}$$

repeat

Solve for the Cartesian velocities:
- evaluate the coefficients of the transport eq. using 1st ord. Upwind.
- evaluate the Reynolds stresses.

for *u, v, w*
- add in the source the pressure gradient term.
- add in the source the turbulent diffusion term.
- add in the source the deferred correction for the high-order scheme.
- solve the three-dimensional system with GMRES.

next
- update the contravariant velocities *U, V, W.*

Solve for the pressure correction:
- correct the contravariant velocities using the Rhie and Chow scheme.
- evaluate the coefficients and the source (mass unbalance).
- solve the three-dimensional system using the direct solver.
- update the pressure and correct *U, V, W.* Update *u, v, w.*

Solve for the turbulence quantities:
- evaluate the coefficients of the transport eq. using 1st ord. Upwind.
- evaluate the Reynolds stresses.
- evaluate the production of turbulence energy.

for *k,* ε
- add in the source the generation and dissipation terms.
- add in the source the turbulent diffusion term.
- add in the source the deferred correction for the high-order scheme.
- solve the three-dimensional system with GMRES.

next

until convergence.

Figure 1. Flowchart of the procedure.

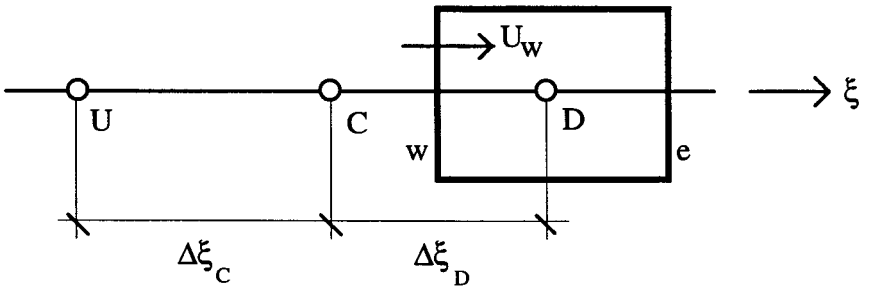

Figure 2. Typical control volume.

6. RESULTS OF THE NUMERICAL TESTS

The solution procedure described in the previous sections has been tested for the turbulent water flow analysis inside a three-dimensional duct of square cross section (40×40 mm) with a 90° bend, as illustrated in Figure 3. The geometry of the duct and the value of the inlet velocity were the same as those used in the experimental measurements of Taylor *et al.* [27]. A characteristic of the flow in this bend is the generation of strong streamwise vorticity, or secondary motion, within the duct, which results in large redistribution of streamwise velocity. The influence of the secondary motion on the streamwise velocity distribution is particularly evident towards the exit of the bend, with the position of maximum velocity migrating towards the outer wall. The experimental data for the turbulent fields show higher shear stress towards the outer radius and large anisotropy at the exit of the bend, with high gapwise normal Reynolds stresses near the pressure surface (outer wall) and high streamwise normal Reynolds stresses near the suction surface (inner wall, or wall towards the centre of curvature).

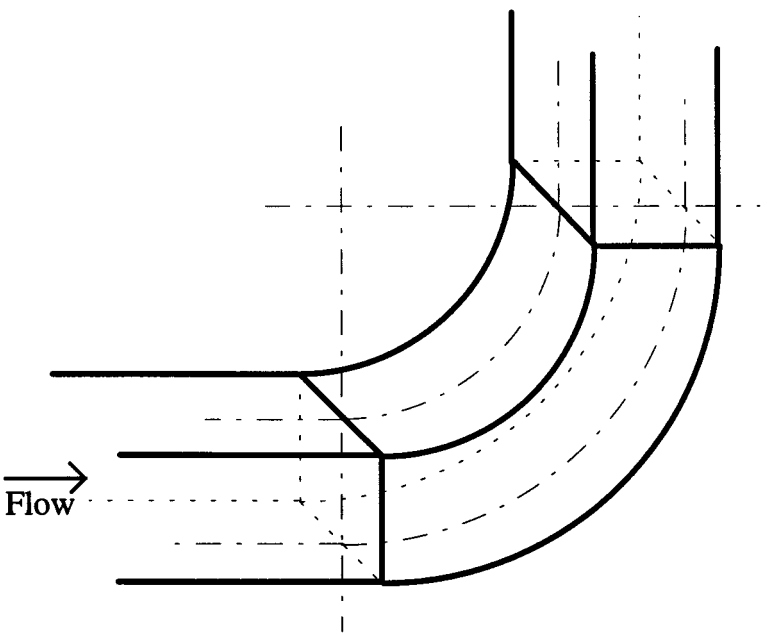

Figure 3. The 90° square section bend.

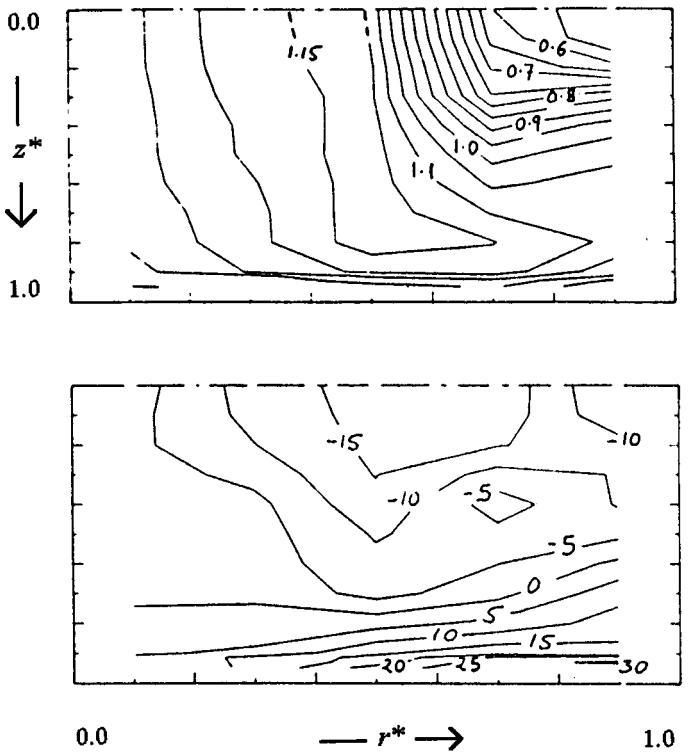

Figure 4. Isotachs of the measured values of U/U_b (top) and V/U_b (bottom), taken from Taylor *et al.* [27].

The duct has been discretised with a $20 \times 20 \times 100$ grid, with the grid points close to the wall in a complete turbulent region ($y^+ \approx 25$ for all the walls in all the domain). The number of points in the cross sections can be considered to be sufficient for the description of the large secondary motions generated at the exit of the bend. The value of the underrelaxation coefficients used is 0.1 for all of the transport equations and for the pressure correction.

All of the results presented refer to the cross section located at 0.25 hydraulic diameters downstream of the bend exit plane, of which only half is represented, due to the spanwise symmetry of the problem. The streamwise velocity is indicated in the figures by U and gapwise velocity is indicated by V; both velocities have been normalised by the bulk velocity $U_b = 1.002$ m s^{-1} (corresponding to $Re = 40\,000$), and the gapwise velocity has been multiplied by a factor of 100. The results are given as a function of the distance from the plane of symmetry normalised by the duct half-span, z^*, and of the distance from the outer wall normalised by the duct gap, r^*.

The isotachs of the measured [27] streamwise and gapwise velocities are represented in Figure 4.

The isotachs of the values of U/U_b calculated with the non-linear modelling of the Reynolds stresses using the QUICK scheme, for several values of the constant C, are represented in Figure 5. For $C = 0.002$, an increase of the velocity towards the pattern present in the measured data is observed (line $U/U_b = 1.15$); increasing the constant to $C = 0.004$, both the lines $U/U_b = 1.15$ and 1.1 reach a position very close to the corresponding lines in the measured data (Figure 4). A further increase of the constant to $C = 0.006$ does not produce additional effects. The value $C = 0.004$ is therefore adopted; note that this value is very close to the one proposed by Baker and Orzechowki for their model.

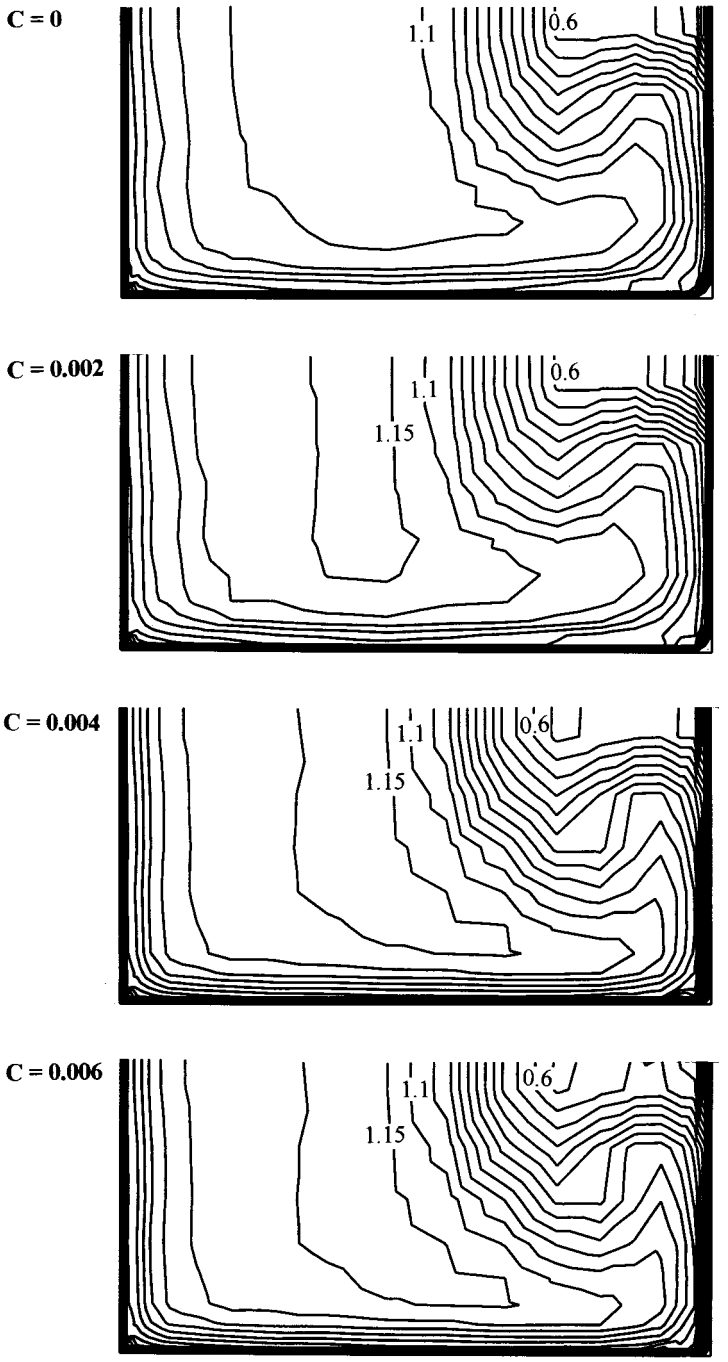

Figure 5. Isotachs of the values of U/U_b calculated with the quadratic modelling of the Reynolds stresses for several values of the constant C, using the QUICK scheme.

The isotachs of the values of V/U_b calculated with the non-linear modelling of the Reynolds stresses using the QUICK scheme, for several values of the constant C, are represented in Figure 6. In this case the effects of the non-linear term can be clearly observed in the shape of the line $V/U_b = -10$ that, for $C = 0.004$, reaches a position very similar to the corresponding line in the measured data. Also in this case, an increase in the value of the constant does not produce additional effects.

If a first-order upwind scheme is used for the treatment of the convection, a small increase in the value of the streamwise velocity is observed for the much higher value $C = 0.01$ (Figure 7), while no effect can be observed on the gapwise velocity (Figure 8).

The results obtained using the non-linear turbulence model with $C = 0.004$ and the three-dimensional QUICK scheme for the treatment of the convection will be presented below.

The streamwise velocity profiles obtained with the different methods (where the proposed formulation is referred to as the 'modified' formulation), soon before and soon after the exit of the bend, are represented in Figures 9 and 10. The profiles obtained with a linear eddy viscosity formulation, adopting the same solution procedure and the same convection scheme, and are also represented in these figures. The effects of the different modelling of the turbulent diffusion term and the efficacy of the quadratic correction introduced in the Reynolds stresses can easily be observed, particularly close to the inner wall ($r^* = 0.9$).

At the exit of the bend the non-linear model causes the movement of the position of the minimum value of the pressure towards the plane of symmetry, while the value itself increases in absolute value. This effect corresponds to the movement, although small, of the centre of the secondary vortex towards the symmetry plane and an increase in the intensity of the secondary flows, while the secondary flows in the rest of the downstream section appear to be unaffected (Figure 11).

The comparison with the available measured data also shows an improvement in the prediction of the pressure field, as can be observed in Figures 12 and 13, where both streamwise and gapwise distributions of the non-dimensional pressure coefficient Cp, defined as

$$Cp = \frac{P - P_{\text{ref}}}{\frac{1}{2}(\rho U_b^2)},$$

where P_{ref} is the pressure at the bend entry on the wall of the suction side of the bend in the plane of symmetry, are represented for the pressure side of the bend.

The authors do not have the computer power to considerably increase the size of the grid, as necessary to study the grid independence of the solution with the presented algorithm, but the use of a higher order scheme, such as Equation (11), should drastically reduce such a dependence. Tamamidis and Assanis [28] have studied the effects of higher order schemes on the prediction of the laminar and turbulent flow in the same 90° bend, using a linear eddy viscosity formulation. They have shown that grid independence is actually obtained in this case using either a third- or fifth-order one-dimensional convection scheme with a similar number of points in the cross sections (22×22).

Figure 14 shows the convergence history of the maximum value of the mass unbalance for both convection schemes. The effect of the accurate solution of the pressure correction equation can be seen in the rapid drop of the mass unbalance, that decreases by several orders of magnitude in less than 100 steps. The oscillatory behaviour of the results obtained with the QUICK scheme is due to the use of the flux limiter, which also affects the minimum value of residuals achievable by the procedure. The residuals of the transport equations follow an identical pattern.

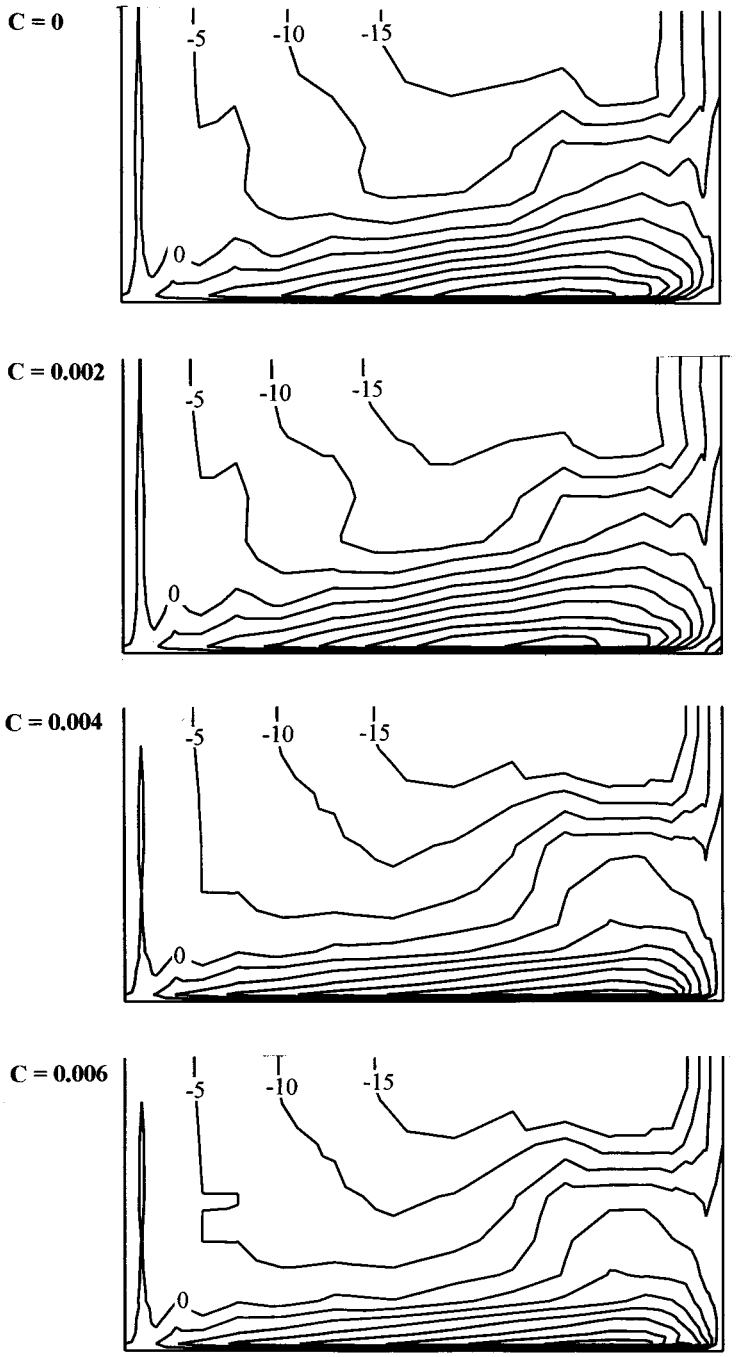

Figure 6. Isotachs of the values of V/U_b calculated with the quadratic modelling of the Reynolds stresses for several values of the constant C, using the QUICK scheme.

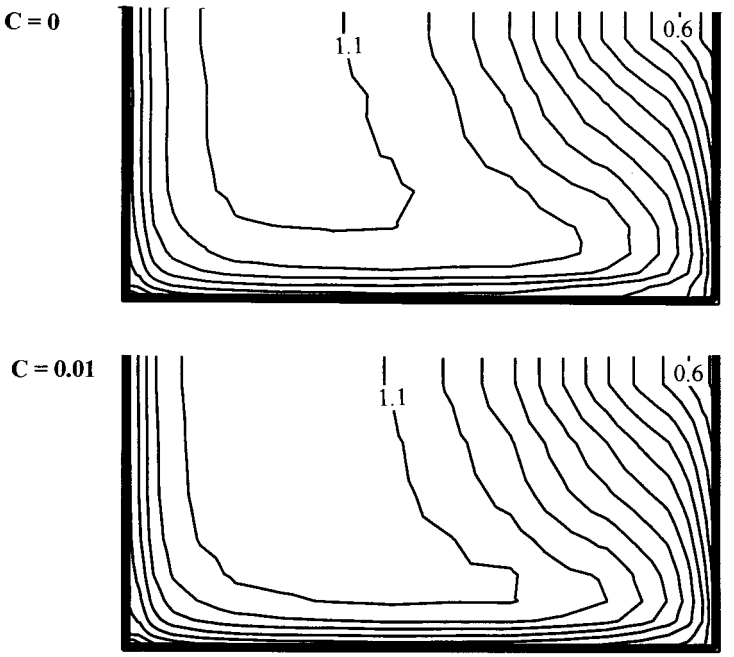

Figure 7. Isotachs of the values of U/U_b calculated with the quadratic modelling of the Reynolds stresses for two values of the constant C, using the first-order upwind scheme.

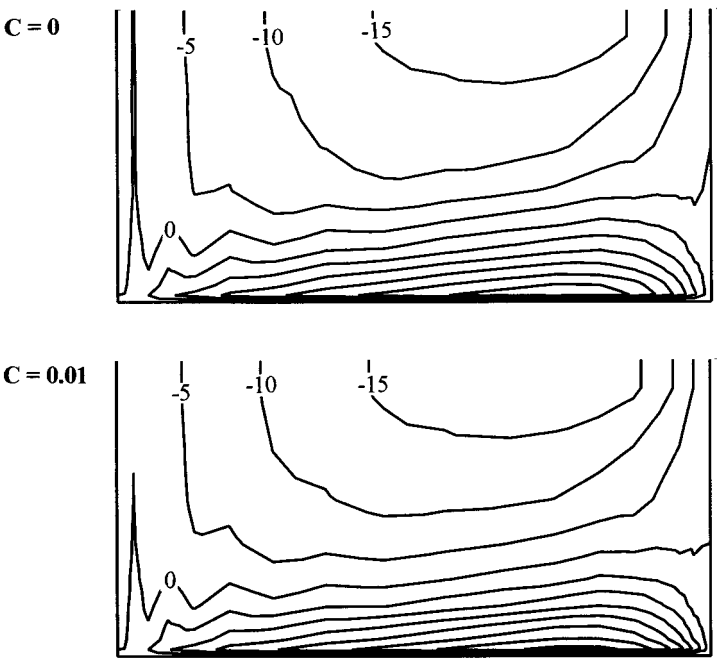

Figure 8. Isotachs of the values of V/U_b calculated with the quadratic modelling of the Reynolds stresses for two values of the constant C, using the first-order upwind scheme.

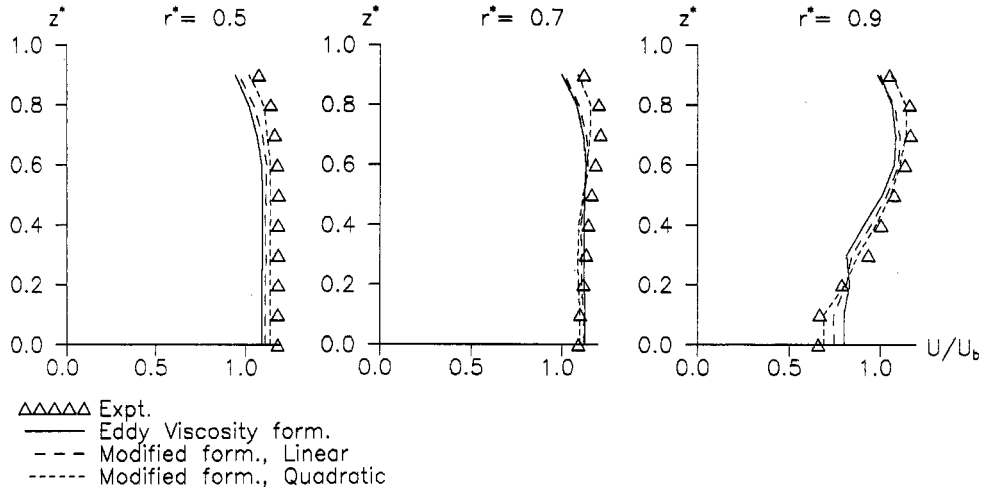

Figure 9. Comparison with the measured data of the streamwise velocity profiles calculated with the different formulations using the QUICK scheme, at 77.5° from the bend entry plane.

Finally, an indication of the CPU time and memory locations required by the procedure is given in Tables I and II. As could be expected, the direct solver severely affects both the CPU time and the memory needed by the procedure.

7. CONCLUSIONS

A modified k–ε method, based on a more accurate modelling of the diffusion term, has been tested on a three-dimensional case in conjunction with a non-linear modelling of the Reynolds stresses. The results presented show that the introduction of a quadratic term in the modelling of the Reynolds stresses delivers a much more accurate prediction of the flow, both for the velocity and the static pressure.

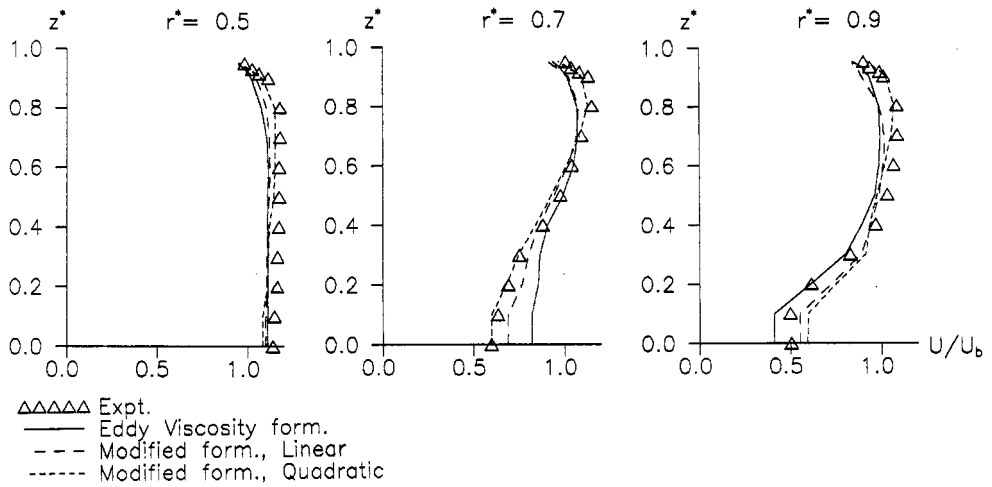

Figure 10. Comparison with the measured data of the streamwise velocity profiles calculated with the different formulations using the QUICK scheme, at 0.25 hydraulic diameters downstream of the bend exit plane.

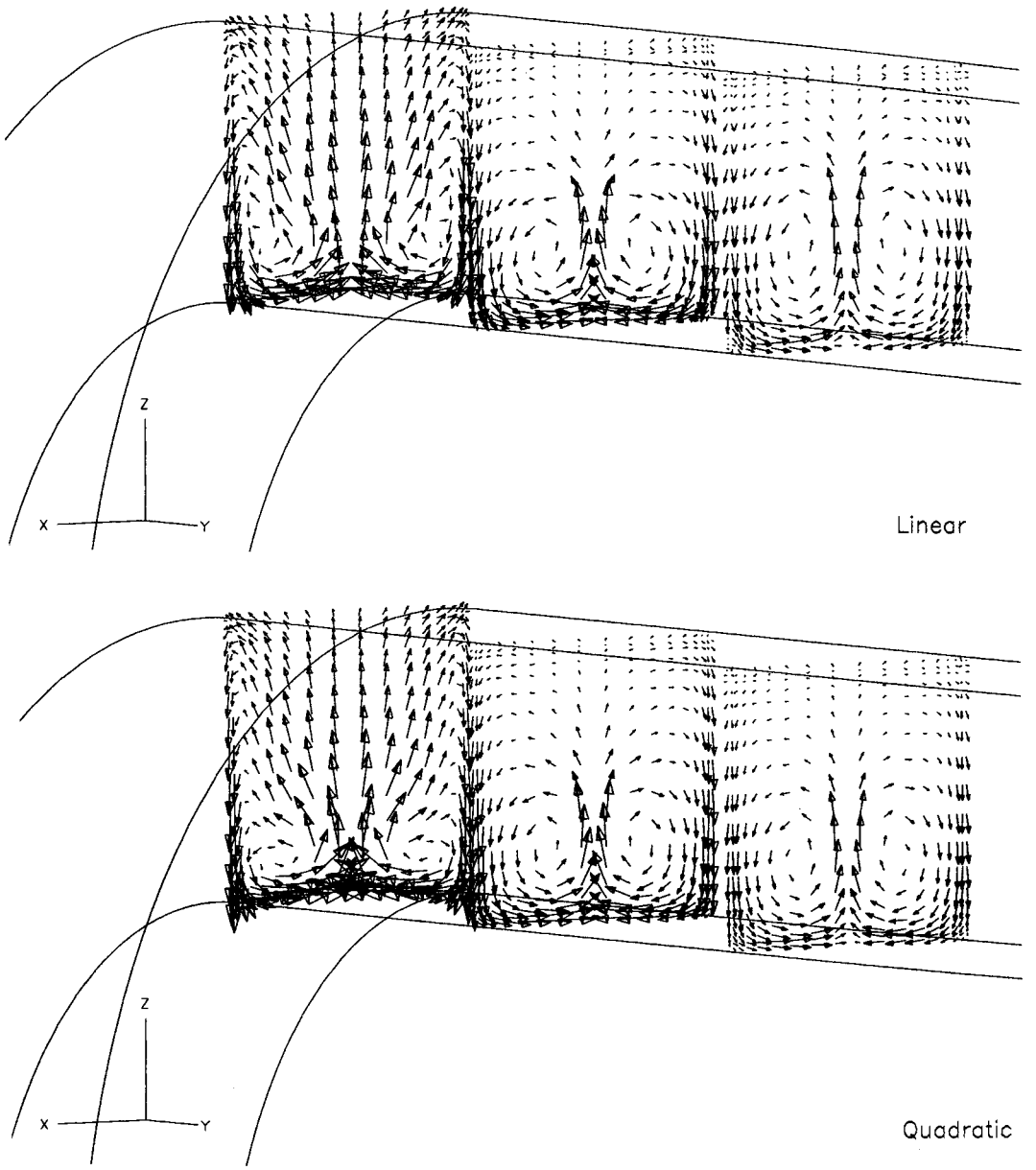

Figure 11. Secondary flows at the exit of the bend calculated using the linear modelling of the Reynolds stresses (top) and the quadratic modelling (bottom).

Although the results presented for the 90° bend show that the simple quadratic correction introduced in the modelling of the Reynolds stresses allows a very close prediction of the streamwise velocity profiles, therefore contributing positively to the resolution of both the anisotropy in the turbulence introduced by the bend and the effects of streamline curvature on the stresses, with difficulty, the proposed modelling (9) can be seen as an universal formulation for the Reynolds stresses, while the modelling constant C cannot be defined by this single test alone.

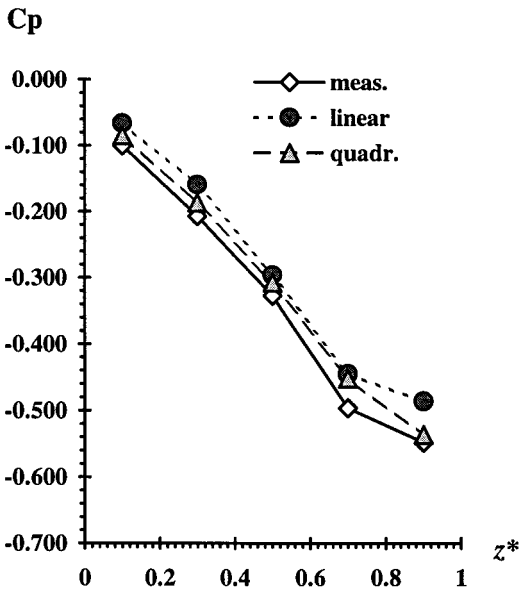

Figure 12. Gapwise distribution of the pressure coefficient *Cp* on the wall on the pressure side of the bend, as function of the distance from the symmetry plane normalised by the duct half-span, at the bend exit plane.

It is interesting to note that increasing the value of the constant C, even doubling it, shows no difference in the results, while much higher values of C cause the complete divergence of the procedure. At the same time, a comparison with some of the other non-linear models proposed in the literature seems to suggest a much higher value of the modelling constant than the one used in the previous section.

As the introduction of additional terms in the modelling of the Reynolds stresses appears to cause a further deterioration in the stability of the procedure, the authors believe that, for three-dimensional applications, the choice of the formulation for the Reynolds stresses should also be made on the basis of considerations of stability and 'practicality'. Convergence with

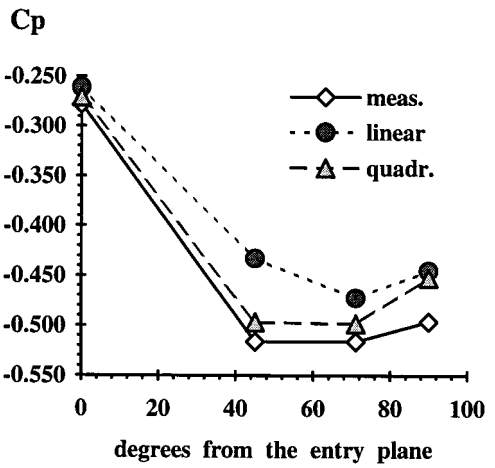

Figure 13. Streamwise distribution of *Cp* on the wall on the pressure side of the bend at 0.7 half-span from the symmetry plane.

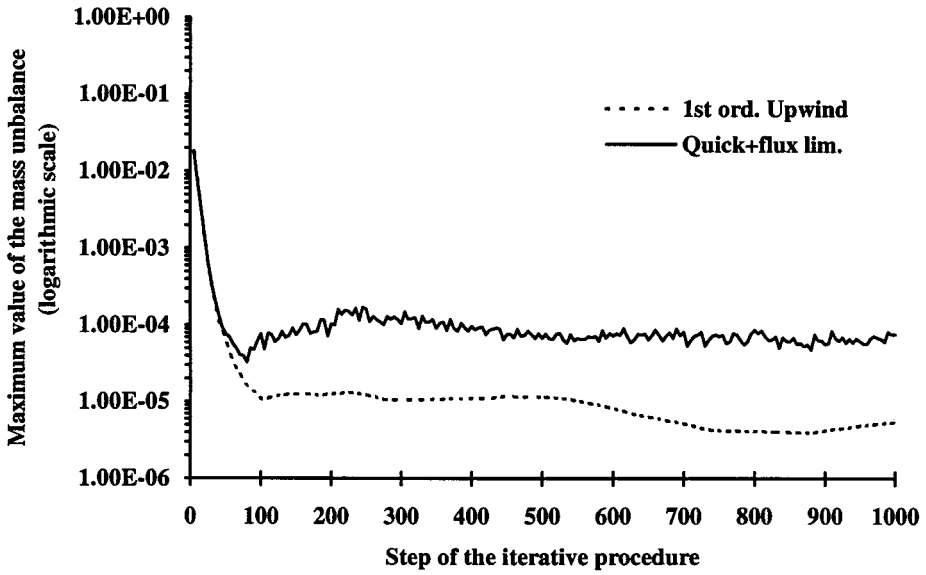

Figure 14. Convergence history of the procedure for the two convection schemes.

Reynolds stresses formulations designed to represent a large number of more or less complex flows could prove to be impossible for same case, while the introduction of simple ad hoc corrections, as in this study, could lead to a sharp improvement in the prediction without an excessive computational cost.

Table I. CPU time for a single step of the procedure (Cray J-90)

Subroutine	Time (s)	Percentage (%)
Total time for one step	40	
Solution of the pressure correction equation	31.1	77
Solution of all the transport equations	2.6	6.6
Evaluation of turbulent diffusion term for k	0.22	0.55
Evaluation of turbulent diffusion term for ε	0.05	0.12
High-order scheme	0.11	0.28
Flux limiter	0.27	0.67

Table II. Memory locations required by the procedure

	Memory locations	Percentage (%)
Total	$\approx 10 \cdot 10^6$	
Direct solver	$\approx 11 \cdot 10^6$	68
Metric coefficients and geom. quant.	$\approx 2.4 \cdot 10^6$	15
All variables and Reynolds stresses	$\approx 5.2 \cdot 10^6$	3
Coefficients, values of the variables in the comp. space, on the cell faces, etc.	$\approx 1.6 \cdot 10^6$	10

Furthermore, as has been partially seen in this study, numerical diffusion plays an important role in the choice of the modelling constant; some of the values obtained in the previous works through computer optimisation could therefore depend on the convection scheme adopted, while the values proposed for stress–strain relationships calibrated through eddy viscosity formulations could be severely affected by the excessive numerical diffusions introduced by the simplified modelling of the turbulent diffusion term, as in Equation (1). It is clear that there is much more work to be done in this field.

In the form presented for the modified k–ε method, any modelling of the Reynolds stresses can be directly adopted in a completely general formulation, while keeping the simple formulation of the standard k–ε method. The formulation presented is effectively an attractive alternative to second-order closure methods, that require a much larger computational effort, while, in respect to non-linear eddy viscosity methods, it provides a better modelling of the turbulent diffusion and a more direct way of adopting different modellings of the Reynolds stresses.

For practical three-dimensional computations the proposed formulation can be written as a correction to a linear eddy viscosity formulation, e.g. for the k equation

$$\frac{1}{J}\frac{\partial}{\partial \xi_r}(\rho U_r k) = \frac{1}{J}\frac{\partial}{\partial \xi_r}\left[J\left(\mu + \frac{\mu_t}{\sigma_k}\right) g^{rs}\frac{\partial k}{\partial \xi_s}\right] + G - \rho\varepsilon + \frac{1}{J}\frac{\partial}{\partial \xi_r}\left[JC_s\frac{k}{\rho\varepsilon}\frac{\partial \xi_r}{\partial x_j}\left(\tau_{il}^R\frac{\partial \xi_s}{\partial x_l}\frac{\partial \tau_{ij}^R}{\partial \xi_s} - \rho\tau_{jl}^R\frac{\partial \xi_s}{\partial x_l}\frac{\partial k}{\partial \xi_s}\right) - J\frac{\mu_t}{\sigma_k}g^{rs}\frac{\partial k}{\partial \xi_s}\right], \tag{13}$$

where the last term, representing the correction, is added in the source. In this form the proposed formulation can easily be included as an additional source term in existing three-dimensional codes.

It is useful to point out that, although presented for a relatively simple case, the main area of application of this method by the authors is the prediction of the turbulent flow field in rotating turbomachinery passages, such as centrifugal pumps and compressors. Written in the form of Equation (13) the proposed method appears to be sufficiently stable to guarantee convergence for most turbomachinery applications, and is currently being used for computations of engineering interest.

APPENDIX A. NOMENCLATURE

C_p	pressure coefficient
C_μ, C_s, C_ε, $C_{\varepsilon 1}$, $C_{\varepsilon 2}$, C	turbulence modelling constants
D_{ij}	twice the mean strain rate tensor $= (\partial u_i/\partial x_j) + (\partial u_j/\partial x_i)$
g^{rs}	metric coefficients $= (\partial \xi_r/\partial x_i)(\partial \xi_s/\partial x_i)$
G	production of k
J	Jacobian
k	turbulent kinetic energy
$\underline{k}$	direction of the z-axis
P	static pressure; also: node at the centre of the control volume
r^*	normalised distance from the outer wall of the bend
S_P	source term in the system of linear equations
u_i, u, v, w	mean Cartesian velocity components

u_i'	fluctuating Cartesian velocity components
U_i, U, V, W	contravariant velocity components, $U_i = J(\partial\xi_i/\partial x_j)u_j$; also: U = streamwise velocity, V = gapwise velocity
U_b	bulk velocity
$\underline{V}$	mean Cartesian velocity vector
x_i, x, y, z	Cartesian co-ordinates
z^*	normalised distance from the plane of symmetry of the bend

Greek letters

α_K	coefficient of the discretised transport equation
δ_{ij}	Kroneker's delta
$\Delta\xi_C$, $\Delta\xi_D$	distance between grid points in the ξ-direction
$\Delta\eta$, $\Delta\zeta$	cell dimension in the η- and ζ-directions
ε	dissipation rate of k
μ	molecular viscosity
μ_t	eddy viscosity
ξ_i, ξ, η, ζ	curvilinear (or generalised) co-ordinates
ρ	density
σ_ϕ	turbulent Prandtl number for the variable ϕ
τ_{ij}^R	Reynolds stress tensor $= \rho\overline{u_i'u_j'}$

Subscripts

C	node upstream of the cell face
D	node downstream of the node C
e	east face of the control volume
P	node at the centre of the control volumes
U	node upstream of the node C
w	west face of the control volume
W, E, S, N, F, B	nodes preceding and following the node P in the ξ-, η- and ζ-directions

REFERENCES

1. W.P Jones and B.E. Launder, 'The prediction of laminarization with a 2-equation model of turbulence', *Int. J. Heat Mass Transf.*, **15,** 301 (1972).
2. B.E. Launder and D.B. Spalding, 'The numerical calculation of turbulent flows', *Comput. Methods Appl. Mech. Eng.*, **3**, 269 (1974).
3. F.S. Lien and M.A. Leschziner, 'A general non-orthogonal collocated finite volume algorithm for turbulent flow at all speeds incorporating second-moment turbulence-transport closure, Part 1: Computational implementation', *Comput. Methods Appl. Mech. Eng.*, **114**, 123 (1994).
4. B. Lakshminarayana, 'Turbulence modelling for complex shear flows', *AIAA J.*, **24**, 1900 (1986).
5. K. Hanjalic and B.E. Launder, 'A Reynolds stress model of turbulence and its application to thin shear flows', *J. Fluid Mech.*, **52**, 609 (1972).
6. A.J. Baker and J.A. Orzechowski, 'An interaction algorithm for three-dimensional turbulent subsonic aerodynamic juncture region flow', *AIAA J.*, **21**, 524 (1983).
7. C.G. Speziale, 'On nonlinear k–l and k–ε models of turbulence', *J. Fluid Mech.*, **178**, 459 (1987).
8. P. Bradshaw, 'The effects of streamline curvature on turbulent flow', *AGARDograph* 169 (1973).
9. A. Melling and J.H. Whitelaw, 'Turbulent flow in a rectangular duct', *J. Fluid Mech.*, **78**, 289 (1976).
10. C.G. Speziale, 'On turbulent secondary flows in pipes of non-circular cross-section', *Int. J. Eng. Sci.*, **20**, 863 (1982).
11. S. Nisizima and A. Yoshizawa, 'Turbulent channel and Couette flows using an anisotropic k–ε model, *AIAA J.*, **25**, 414 (1987)
12. R. Rubinstein and J.M. Barton, 'Non-linear Reynolds stress models and renormalization group', *Phys. Fluids A*, **2**, 1472 (1990).

13. H.K. Myong and N. Kasagi, 'Prediction of anisotropy of the near wall turbulence with an anisotropic low-Reynolds-number $k-\varepsilon$ turbulence model, *J. Fluids Eng*., **112**, 521 (1990).
14. T.H. Shih, J. Zhu and J.L. Lumley, 'A realizable Reynolds stress algebraic equation model', *NASA TM 105993*, 1993.
15. T.J. Craft, B.E. Launder and K. Suga, 'Development and application of a cubic eddy-viscosity model of turbulence', *Int. J. Heat Fluid Flow*, **17**, 108 (1996).
16. F.S. Lien and M.A. Leschziner, 'Assessment of turbulence-transport models including non-linear RNG eddy-viscosity formulation and second-moment closure for flow over a backward-facing step', *Comput. Fluids*, **23**, 983 (1994).
17. C.G. Speziale, 'Closure models for rotating two-dimensional turbulence', *Geophys. Astrophys. Fluid Dyn*., **23**, 69 (1983).
18. J. Laufer, 'Investigation of turbulent flow in a two-dimensional channel', *NACA TN 1053*, 1952.
19. S.V. Patankar, *Numerical Heat Transfer and Fluid Flow*, Hemisphere, Washington DC, 1980.
20. C.M. Rhie and W.L. Chow, 'Numerical study of the turbulent flow past an airfoil with trailing edge separation', *AIAA J*., **21**, 1525 (1983).
21. Y. Saad and M.H Schultz, 'GMRES: a generalized minimal residual algorithm for solving non-symmetric linear system', *SIAM J. Sci. Comput*., **7**, 856 (1986).
22. V. Botte, A. Tourlidakis and R.L. Elder, 'Influence of the convection scheme on the solution of the pressure correction equation using GMRES with short restart', in F. Benkhaldoun and R. Vilsmeier (eds.), *Finite Volumes for Complex Applications*, Hermes, Paris 1996, pp. 417–424.
23. J.W. Liu, 'Modification of the minimum degree algorithm by multiple elimination', *ACM Trans. Math. Softw*., **11**, 141 (1985).
24. J.W. Liu, 'The multifrontal method for sparse matrix solution: theory and practice', *SIAM Rev*., **34**, 82 (1992).
25. B.P. Leonard, 'Elliptic systems: finite difference method IV', in W.J. Minkowycz *et al*. (eds.), *Handbook of Numerical Heat Transfer*, Wiley, New York, 1988, pp. 347–378.
26. P.H. Gaskell and A.K.C. Lau, 'Curvature-compensated convective transport: SMART, a new boundedness-preserving transport algorithm', *Int. J. Numer. Methods Fluids*, **8**, 617 (1988).
27. A.M.K. Taylor, J.H. Whitelaw and M. Yianneskis, 'Measurements of laminar and turbulent flow in a curved duct with thin inlet boundary layers', *NASA Contractor Report 3367*, 1981.
28. P. Tamamidis and D.N. Assanis, 'Three-dimensional incompressible flow calculations with alternative discretisation schemes', *Numer. Heat Transf. Part B*, **24**, 57 (1993).

